American Meteorological Society
32nd Radar Meteorology Conference
October 2005, Albuquerque, NM

P14R.4

Z-R RELATIONS FROM RAINDROP DISDROMETERS: SENSITIVITY TO REGRESSION METHODS AND DSD DATA REFINEMENTS

Brooks E. Martner[1,2], Vladimir Dubovskiy[1,3], and Sergey Y. Matrosov[1,2]

[1] = NOAA Environmental Technology Laboratory, Boulder, CO
[2] = CIRES, University of Colorado, Boulder, CO
[3] = Science & Technology Corp., Boulder, CO

1. Introduction.

Most radar estimations of rainfall intensity and accumulations are still based on empirical relations between rainfall rate R (in mm/h) and reflectivity factor Z (in mm^6m^{-3}). In many cases these Z-R relations are derived from drop size distributions (DSDs) measured by raindrop disdrometers. Regressions are fit to the scatter of (Z,R) points to determine the relation, which is almost always stated as $Z = aR^b$. The well-known table by Battan (1973) lists dozens of examples of early Z-R equations from researchers in various parts of the world, with the implication that the equation differences are attributable to different types of rainfall processes. Scores of additional relations have been published since then.

However, recent studies by Ciach and Krawjewski (1999), Campos and Zawadzki (2000), and Tokay et al. (2001) point out that Z-R equations are method dependent. The same dataset may provide markedly different values of *a* and *b* when the regression is manipulated in different ways. These method-dependent Z-R differences might even be larger than those obtained from truly physically different rainfall regimes and may account for much of the abundant dispersion in Z-R equations reported in the literature.

Author contact: Brooks Martner, NOAA/ETL, 325 Broadway, Boulder, CO 80305.
E-mail: brooks.martner@noaa.gov

In this study we further quantify the effect that several common regression processing options and DSD data refinements have on the Z-R relations. We compare these method-dependent differences with Z-R differences obtained using the same procedures for two geographically and physically different storm types. Our data are from a single drop-momentum-sensing disdrometer (JWD), originally described by Joss and Waldvogel (1967). This JWD was operated on the prairie in Colorado and on the coastline in northern California. The spring and summer rainfall sampled in Colorado was primarily from deep convective storms. In contrast, the rain in California fell from shallow, stratiform winter storms. In the California case, the disdrometer data only included raining periods when no melting-layer bright band was observed aloft by a collocated S-band profiling radar. Storms during these periods contain no snowflakes or large ice crystals aloft and are usually characterized by shallow echo tops, an abundance of small drops, and few large drops (White et al 2003).

We examined the effects on the resulting Z-R equations of three common processing options (and combinations of them) that represent essentially arbitrary choices for the analyst's use of the (Z,R) points. We also examined the effects of five refinements to the DSD data, some of which are unique to the JWD kind of disdrometer. These methodology choices are shown in Table 1.

Table 1. Method-Dependent Choices Investigated in this Study.

Processing Options choice of:	**Comment**
Dependent variable	R or Z
Cutoff threshold	R>0.1 mm/h, R> 1 mm/h, or Z > 15 dBZ
Regression type	linear fit to log-R vs log-Z or power law fit to R vs Z
Refinements use of:	**Comment**
Instrument-specific bin/size calibration*	instead of nominal calibration
Dead-time corrections (dtc) to DSD*	Sheppard and Joe (1994)
Time integration for DSDs	1 min or 10 min (with dtc)
Altitude adjustments to drop fall speeds and momentum/diameter relations	instead of sea-level values
Non-Rayleigh Z values appropriate for X-band radar observations	instead of $Z = \sum nD^6$

* = unique to JWD disdrometers

2. Common Processing Options.

Although Z-R relations are traditionally stated as Z=f(R), the choice of dependent variable is arbitrary for disdrometer data. From a practical point of view, however, the equations are most often inverted to get R=f(Z), because radar observations of Z are available and their conversion to unknown values of R is desired. Thus, R is a more practical choice for the dependent variable. The choice matters because standard regression fitting algorithms minimize the distance of the fit line from the points in the y-axis (dependent variable) direction and the results are different if the variables are reversed. Lee and Zawadzki (2005) use a more sophisticated procedure, unavailable in most commercial regression software, which minimizes the perpendicular distance of the points to the regression line, thereby, avoiding the differences arising from the choice of dependent variable.

Disdrometers such as the JWD are capable of recording tiny rain rates and reflectivities from a few individual drops, but these points have no practical value and are subject to large statistical and instrumental uncertainties. Thus, it is common practice to exclude all points below some arbitrary lower cutoff threshold. Using R > 0.1 mm/h, for example, limits the data included in a regression fit approximately to drizzle and stronger rain. Using R> 1 mm/h limits the data to light and stronger rain. Using a Z threshold, such as Z > 15 dBZ, has the practical advantage of being directly applicable to a field of observed radar pixels. Setting any of these thresholds too high, however, leaves a small population of relatively clustered points and results in a low correlation value and decreased confidence for the regression.

Nearly all earlier Z-R equations were computed using simple linear least-squares-fit regressions to the scatter of log-R and log-Z data points. Modern software packages now make more sophisticated regressions convenient to use, such as a two-parameter power law fit directly to the R and

and Z points. But the linear and non-linear fits to exactly the same data produce different regression equations because of the nature of the fitting algorithms. According to Campos and Zawadzki (2000), power law regression fits to R vs Z represent rain accumulations better and linear fits to log-R vs log-Z represent instantaneous rain rates better.

3. Available Refinements to the DSD data.

The JWD disdrometer is manufactured by Distromet, LTD, in Basel, Switzerland, and is delivered with software that computes R and Z from the observed DSD for each sample time increment (typically 1 min). These "raw" Z and R values are computed assuming a nominal calibration of the D values for each of 20 size bins (spanning approximately 0.4 to 5.3 mm), interpolated from a finer-resolution set of 127 size bins. However, the manufacturer also provides a table of more precise calibration data specific to the individual disdrometer purchased. In our case, these calibrated D values differed from the nominal values by 0-2%, but most differed by less than 1%. The raw values also assume the impacting drops have momentums appropriate for their terminal velocities at sea level and that Z is for Rayleigh scattering conditions, such as would be appropriate for observing rain with S-band radar. This may lead to errors for data collected at high altitudes where fall speeds are larger, and for applications using shorter wavelength radars, such as X, Ku, or Ka-band. The JWD disdrometer employs a dead-time interval between recorded drops which excludes counting pulses from sensor ringing and helps avoid counting satellite splash drops. However, the dead-time interval also causes the instrument to miss counting *bona fide* drops that hit the sensor in rapid succession. Shepard and Joe (1994) show a dead-time correction (dtc) equation that partially corrects the recorded raw DSD for this factor. For convenience, many analysts use the raw JWD data as is, off the shelf, without regard to the possible effects of these refinements.

Disdrometer users must also select their recording interval; 1 minute is typically used. However, longer sample accumulation times (applied during data collection or afterwards), such as 10-min intervals used by Hagen and Yuter (2003) have the advantage of reducing DSD statistical uncertainties and an inherent biasing of Z-R equations, by increasing the number of drops in each bin (Smith et al. 1993). In the method of Lee and Zawadzki (2005), 1-minute DSD data from several hours of rainfall are sorted and grouped together by their Z (or R) values and 10 or more of these discontinuous minutes of DSDs are subjected to a moving average to produce filtered DSDs. The resulting (Z,R) points from the filtered DSD data exhibit greatly diminished scatter compared to the raw 1-minute data points.

4. Data and Methods.

DSD data were collected with a JWD on the prairie near Erie, Colorado (1587 m MSL) from May to July 2004 as part of NASA's Global Precipitation Measurement (GPM) program. The same disdrometer also sampled winter rainfall on northern California's coast at Bodega Bay (12 m MSL) as part of NOAA's Hydrometeorology Testbed (HMT) program from December 2003 to March 2004. All of the Colorado data from 18 stormy periods were used in this study. Most were convective storms, but one period of light stratus rain was included. The California data used in this study included only those rainy half-hour periods for which a collocated S-band profiler observed no bright band aloft, according to the objective criteria of White et al (2003). As such, the Colorado data included far more short periods of intense rain from deep clouds, while the California data were characterized by generally lighter rain rates from shallower clouds.

5. Storm-type/Location Difference.

The DSD data from each location were initially processed with the following choices to produce a reference Z-R equation for comparison with those obtained at the same location using other method choices. The options selected for the reference equation were: no data refinements (using the raw Distromet output file Z and R values), R as the dependent variable, threshold of R > 0.1 mm/h, 1-minute sampling, and linear regression. The resulting reference equations are:

$$Z = 185R^{1.90} \quad \text{for GPM-Colorado,}$$

and

$$Z = 85R^{1.58} \quad \text{for HMT-California.}$$

The equations are indeed quite different, and because the same instrument and processing were used, we presume the difference reflects a true contrast in the disparate character of the precipitation sampled at these locations. The data from both locations are shown in Figure 1 for the reference processing condition. Although the points overlap extensively, there is noticeable separation of the two populations for reflectivities above about 25 dBZ, where the differences are quite pronounced. At 35 dBZ the predicted rainfall intensities differ by more than a factor of 2, with R= 4.5 mm/h for the GPM-Colorado relation and 9.9 mm/h for the HMT-California relation. The rms difference for the two equations is 6.7 mm/h, using the full population of Z points from both datasets. This number will be compared with the rms differences for the cases where processing options and data refinements are varied.

6. Differences for Various Regression Processing Options

Scatter plots and regressions for the GPM-Colorado data are presented in this section for the several different processing and refinement methods. The HMT-California data received exactly the same treatments, but the graphs are not shown. The Colorado data for the reference case are plotted in Figure 2. The threshold of R> 0.1 mm/h left 3190 points of 1-minute samples for regression. R was selected as the dependent variable and the regression is a linear fit to the log-R vs log-Z data. As shown on the graph, the correlation coefficient, r, for the regression is 0.90. The linear clustering of points along the left side of the plot below R = 2 mm/h are light rain and drizzle points from the only stratus case in the GPM-Colorado dataset.

Figure 3 shows the effect of raising the cutoff threshold to R > 1 mm/h and Figure 4 shows the effect of setting the threshold at Z > 15 dBZ. In Figure 5, Z was chosen as the dependent variable and the cutoff was again set at R > 0.1 mm/h. Figure 6 shows the effect of using a 2-parameter power law regression fit to the R vs Z data with the cutoff again set at R > 0.1 mm/h. The power law fit was computed with the commercial SigmaPlot graphics software for PCs and confirmed with the commercial Grapher and IDL software. In Figure 7, the same kind of power law fit is shown for the regression of Z on R (Z as the dependent variable) with a markedly different result. In this case, the largest few R-value points have a dominating effect on the fit, and the resulting strange-looking Z-R equation differs greatly from all the other regressions.

7. Differences for Various Refinements to the DSD Data.

The effects of applying various refinements to the raw data of the Distromet output files are illustrated in Figures 8-12. The data in Figure 8 were treated exactly the same as those in the reference situation (Fig. 2) except that Distromet’s diameter bin calibrations for this specific instrument were used instead of the nominal calibration. The resulting difference in the regression from that of the reference is slight.

The data in Figure 9 are the same as for the reference, except drop fall speeds and the diameter-momentum relation were adjusted for the high altitude (~1600 m) of the Colorado site. At altitude, lower air density allows a raindrop to fall faster than at sea level and to induce a larger voltage signal upon impacting the JWD sensor. However, the resulting Z-R equation is only slightly affected by accounting for this factor.

In Figure 10 the data are the same as in the reference, except the dead-time correction (dtc) algorithm of Sheppard and Joe (1994) was used to adjust the drop concentrations of the DSD. The effect on the resulting regression is small in this case. The same data are used in Figure 11 except that a 10-minute integration or accumulation time is applied before the dtc (hence there are ~1/10th as many points). Here the difference from the reference is more noticeable, but still small.

Data in Figure 12 were treated the same as for the reference, except the Z values of each point were recomputed from the observed DSD for non-Rayleigh conditions at X-band (assuming spherical drops). The result differs only slightly from the reference case regression. However, it should be noted that the non-Rayleigh adjustment to the Z values becomes increasingly significant when the DSDs contain greater proportions of large drops. The differences are notable for DSDs with median diameters greater than about 2.5 mm (Matrosov et al. 2005), as is often the case for heavy convective rainfall.

Figure 13 shows the Z-R relations derived from exactly the same GPM-Colorado dataset using each of the various processing options and refinements. The lines are plotted as R vs log-Z, to emphasize the very large span of retrieved R values, especially above 40 dBZ. For example, the R values at 50 dBZ range from about 20 to 100 mm/h, although only 2 of the 15 relations give R values above 40 mm/h.

Exactly the same procedures were applied to the HMT data from the non-brightband winter rainfall on California's coastline. The number of data points was quite similar for the two projects, but the HMT-California data were concentrated in lower reflectivities than the GPM-Colorado points. Results for both projects are summarized in Table 2, where the various processing options and refinements are indicated in the five columns on the right side. Although many of the equations within each project appear very different from each other, in some cases the *a* and *b* values have partially offsetting effects. The value of R derived from each regression at Z = 35 dBZ is shown in the table as an illustration of the magnitude of differences among the equations. A root-mean-squared difference (rms difference or standard error) was also computed to assess the variations more thoroughly. Each Z-R equation was paired with the same project's reference equation, and pairs of R values were calculated using the dataset's observed population of Z values (excluding points for which R< 0.1 mm/h) as input. The rms difference for these different method pairs are shown in Table 2. For perspective, recall that the rms difference between the GPM and HMT reference equations was 6.7 mm/h.

Table 2 shows that the individual effects of most of the DSD data refinements (lower portion of Table 2) on the Z-R equation were relatively small. This is illustrated in the GPM data for example, by the values of R at Z=35 dBZ for the refinements, which range from 4.2 to 4.9 mm/h, compared to the 4.5 mm/h reference-equation value. This represents a variation of less than 10%. For HMT, the corresponding variation among the refinements at 35 dBZ is 28%. In contrast, the effect of several of the regression processing options was much greater. For example, simply choosing Z rather than R as the dependent variable and using no other changes, produced R values at 35 dBZ of 6.5 mm/h for GPM (a 44% difference from the reference) and 14.0 mm/h for HMT (a 41% difference from the reference).

The rms differences shown in Table 2 more adequately indicate the overall effects for the entire populations or observed Z values, than just considering a single reflectivity. For both datasets, the greatest rms departures from the reference occurred when using Z as the dependent variable and a cutoff threshold of Z > 15 dBZ. In the GPM data, this 9.1 mm/h rms difference exceeded the 6.7 mm/h rms difference between the reference equations of the two very physically different Colorado and California datasets. Thus, as suggested by Ciach and Krawjewski (1999) and others, arbitrary choices regarding data manipulation can indeed have effects on the Z-R equations that rival or exceed those of physically-based differences between rain processes. The DSD data refinements were less influential in our cases, but were not always negligibly small. Dead-time correction, for example, made one of the lager differences for the HMT dataset.

8. Discussion and Recommendations.

Choices made in how to compute Z-R data regressions and whether to use or ignore various refinements to raw DSD data from disdrometers might seem innocuous. However, they can affect the Z-R relations to a surprisingly large degree, which in some cases is comparable to Z-R equation differences inherent in physically very different rainfall processes. This is a sobering realization. In addition to disdrometer instrumental sources of error, it adds to the well-known sources of uncertainty for radar reflectivity estimates of rainfall, such as radar calibration errors, storm-to-storm DSD variability, contamination of the rain signal by hail, snow, melting snow, or ground-clutter, etc. It provides further motivation for advancing rain estimation schemes beyond those based entirely on radar reflectivity. However, the use of Z-R equations is unlikely to disappear soon. Meanwhile new methods to reduce Z-R uncertainties (*e.g.* Lee and Zawadzki 2005) or to better define those uncertainties will be helpful. Suggestions from our study are offered here for the benefit of future Z-R equation producers and users.

Recommendations Regarding Regression Processing:

1) State the details of your method.
Quite different Z-R relations can be derived from exactly the same data, depending on details of the method used. By stating the processing details, comparisons of Z-R equations from different studies can be more fruitful.

2) Use R as the dependent variable.
The choice of the dependent variable had a relatively large effect on the resulting Z-R equation for our data sets. Although this choice is arbitrary when dealing with disdrometer data, it makes more sense from the viewpoint of practical radar applications to choose R as the dependent variable.

3) Use cut-off thresholds of Z.
Excluding the very light rainfall (Z,R) points below an appropriate threshold will eliminate questionable points that may be contaminated by various sources of noise and have no hydrologic significance. Again, it is more practical to use Z than R as the cut-off threshold when dealing with radar data, and we suggest doing the same for disdrometer data intended for radar applications. The choice of the threshold parameter and its value usually had a moderately large effect on the resulting Z-R equation for our data sets. However, the combination of using Z > 15 dBZ as the cutoff threshold along with selecting Z as the dependent variable (not recommended) produced very large Z-R equation differences for both of our datasets.

4) Use a linear regression to log-R vs log-Z.
Power law fits are heavily weighted by the large-value (R,Z) data points. As such, they may represent accumulations better than rain intensities, but they can be highly skewed by a few such points, which may be of questionable accuracy, far from the main population. This was the case for our GPM

Table 2. Z-R Equations from Disdrometer Data for Two Projects Using Various Processing Options and Data Refinements

	GPM - Colorado			HMT (NBB only) - California			Method Conditions				
	Equation	R rms dif (mm/h)	R at 35 dBZ (mm/h)	Equation	R rms dif (mm/h)	R at 35 dBZ (mm/h)	Refin.	Dep. Var.	Threshold	Regr. Type	Time Accum
Reference:											
1.	$Z = 185R^{1.90}$	0	4.5	$Z = 85\ R^{1.58}$	0	9.9	none	R	R>0.1 mm/h	linear	1 min
Regression Processing Options:											
2.	$Z = 97R^{2.21}$	0.71	4.8	$Z = 44R^{2.07}$	0.89	7.9	none	R	R> 1 mm/h	linear	1 min
3.	$Z = 209R^{1.74}$	1.04	4.8	$Z = 78R^{1.67}$	0.29	9.2	none	R	Z>15 dBZ	linear	1 min
4.	$Z = 174R^{1.55}$	4.81	6.5	$Z = 85R^{1.37}$	1.73	14.0	none	Z	R>0.1 mm/h	linear	1 min
5.	$Z = 160R^{1.70}$	2.47	5.8	$Z = 75R^{1.50}$	0.92	12.1	none	Z	R>1 mm/h	linear	1 min
6.	$Z = 234R^{1.35}$	9.13	6.9	$Z = 100R^{1.24}$	2.80	16.2	none	Z	Z>15 dBZ	linear	1 min
7.	$Z = 142R^{1.86}$	1.05	5.3	$Z = 57R^{1.83}$	0.49	9.0	none	R	R>0.1 mm/h	power	1 min
8.	$Z = 128R^{1.89}$	1.10	5.5	$Z = 46R^{1.93}$	0.61	9.0	none	R	R>1 mm/h	power	1 min
9.	$Z = 5R^{2.63}$	5.49	11.6	$Z = 77R^{1.58}$	0.27	10.5	none	Z	R>0.1 mm/h	power	1 min
10.	$Z = 5R^{2.63}$	5.49	11.6	$Z = 77R^{1.58}$	0.27	10.5	none	Z	R>1 mm/h	power	1 min
Refinements to DSD Data:											
11.	$Z = 170R^{1.88}$	0.36	4.7	$Z = 79R^{1.56}$	0.32	10.6	calib	R	R>0.1 mm/h	linear	1 min
12.	$Z = 170R^{1.91}$	0.15	4.6	n/a	----	---	alt	R	R>0.1 mm/h	linear	1 min
13.	$Z = 152R^{1.92}$	0.38	4.9	$Z = 70R^{1.50}$	1.16	12.7	dtc	R	R>0.1 mm/h	linear	1 min
14.	$Z = 186R^{1.99}$	0.57	4.2	$Z = 81R^{1.59}$	0.08	10.0	dtc	R	R>0.1 mm/h	linear	10 min
15.	$Z = 181R^{1.88}$	0.20	4.6	$Z = 86R^{1.54}$	0.22	10.4	xband	R	R>0.1 mm/h	linear	1 min

calib = using instrument-specific calibration
alt = using altitude corrections
xband = using non-Rayleigh reflectivities for X-band
dtc = using dead time correction

dataset when Z was selected as the dependent variable. The resulting very unusual Z-R equations fit the GPM high-value points well but fit the vastly more common light to moderate rainfall data points poorly. Traditional linear fits to log-R vs log-Z are at less risk of being skewed by a minority of points.

Results Regarding DSD Refinements:

Most of the adjustments to the standard raw Distromet ASCII output files had relatively little effect on the Z-R equations for our two data sets. In the Colorado dataset, all of the regression-processing options (items 2-4 above) were more influential than any of these refinements. The following refinements had trivial or minor impacts on the resulting Z-R equations for both datasets: a) using the specific instrument calibration, b) adjusting drop fall speeds and momentums for 1600-m altitude, and c) adjusting reflectivities for non-Rayleigh conditions appropriate for X-band radar observations. Whereas, applying these refinements makes sense, their trivial effects in our cases suggest they may not be worth the extra effort involved. However, non-Rayleigh effects would certainly be more significant in heavier (large-drop) rain regimes and for shorter wavelengths, and should be included in those situations.

Dead-time correction adjustments to the DSDs showed mixed results for the Z-R relations from our datasets. The effect was minimal for the Colorado data, but relatively large effect for the California non-brightband rain. Thus, the importance of including this refinement is not clearly revealed by this study.

Increasing the sample time integration from 1 to 10 minutes also had rather minor effect for our datasets. In contrast, other studies have emphasized the utility of averaging in time, in R, or randomly. The filtering method of Lee and Zawadzki (2005) impressively reduced their Z-R scatter by averaging 10 or more of the raw 1-minute DSDs, sorted according to their Z values, for long rainfall datasets. However, in dealing with short-lived convective rain, such as most of the Colorado dataset, 10 minutes is on the same order as the typical storm rain duration at a point, and the appropriateness of time averaging schemes must be questioned.

The results presented here may not be representative of other disdrometer datasets. They are offered only as illustrative examples of the magnitude of the effects of various Z-R regression processing options and the application of refinements to raw DSD data from disdrometers. Furthermore, our recommendations relate only to the derivation of Z-R equations and may not be appropriate for other applications, such as characterization of DSD features and relations among other rainfall parameters.

Acknowledgements.

ETL's participation in the GPM Front Range Pilot Project was sponsored by NASA. Scott Abbott of ETL set up the disdrometer for both field projects. We are grateful to Sandra Yuter (University of Washington / North Carolina State University) for the use of her software to compute dead-time corrections and time-integrations of DSD data.

References.

Battan, L.J., 1973: *Radar Observation of the Atmosphere*. Univ. Chicago Press, 324 pp.

Campos, E. and I. Zawadski, 2000: Instrumental uncertainties in Z-R relations. *J. Appl. Meteor.*, **39**, 1088-1102.

Ciach, G.J., and W. F. Krawjewski, 1999: Radar-rain gauge comparisons under observational uncertainties. *J. Appl. Meteor.*, **38**, 1519-1525.

Hagen, M. and S.E. Yuter, 2003: Relations between radar reflectivity, liquid-water content, and rainfall rate during MAP SOP. *Q. J. Royal Meteor. Soc.,* **129**, 477-493.

Joss, J. and A. Waldvogel, 1967: A raindrop spectrograph with automatic analysis. *Pure Appl. Geophys.*, **68**, 240-246.

Lee, G., and I. Zawadzki, 2004: Variability of drop size distributions: Noise and noise filtering in disdrometric data. J. Appl. Meteor., **44**, 634-652.

Matrosov, S.Y., R. Cifellli, P.Kennedy, and B. Martner, 2005: The role of X-band in extending longer-wavelength radar polarimetric retrievals to lighter rainfalls. *32nd Conf. on Radar Meteor*., Albuquerque, NM. (in these proceedings).

Sheppard, B.E., and P.I. Joe, 1994: Comparison of raindrop size distribution measurements by a Joss-Waldvogel disdrometer, a PMS 2DG Spectrometer, and a POSS Doppler radar. *J. Atmos. and Ocean. Tech.*, **11**, 874-887.

Smith, P.L., Z. Liu, and J. Joss, 1993: A study of sampling-variability effects in raindrop size observations. *J. Appl. Meteor.*, **32**, 1259-1269.

Tokay, A., A. Kruger, and W.F. Krajewski, 2001: Comparison of drop size distribution measurements by impact and optical disdrometers. *J. Appl. Meteor.*, **40**, 2083-2097.

White, A.B., P.J. Neiman, F.M. Ralph, D.E. Kingsmill, and P.O.G. Persson, 2003: Coastal orographic rainfall processes observed by radar during the California Land-falling Jets Experiment. *J. Hydrometeor.*, **4**, 264-282.

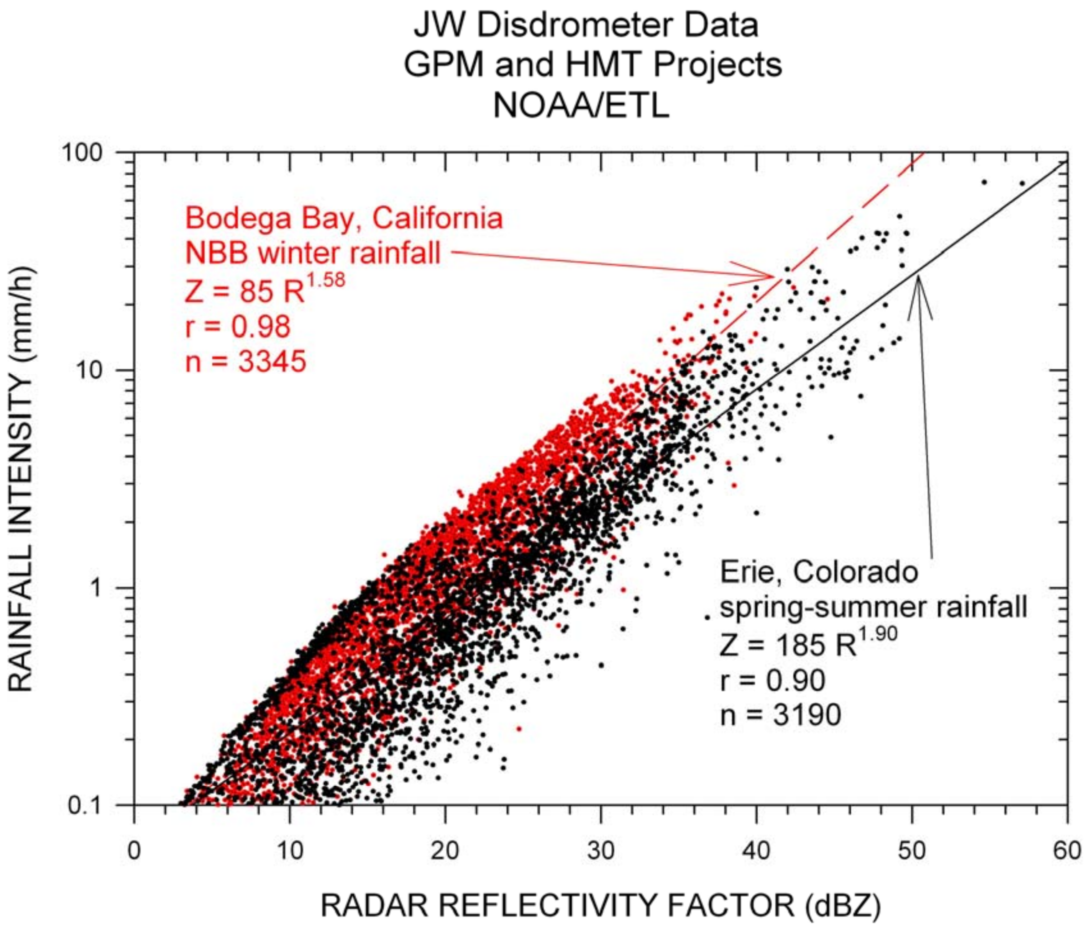

Refinements: None (raw Distromet data)
Thresholding: R > 0.1 mm/h
Dependent Variable: R
Regression: Linear
Time Integration: 1 minute per point

Figure 1. Scatter diagram and Z-R regressions for the GPM04-Colorado rainfall (black) and for the HMT04-Claifornia non-brightband rainfall (red). Each point represents 1 minute of disdrometer data. The number of points (n) and the correlation coefficient (r) of the regressions are shown on the graph.

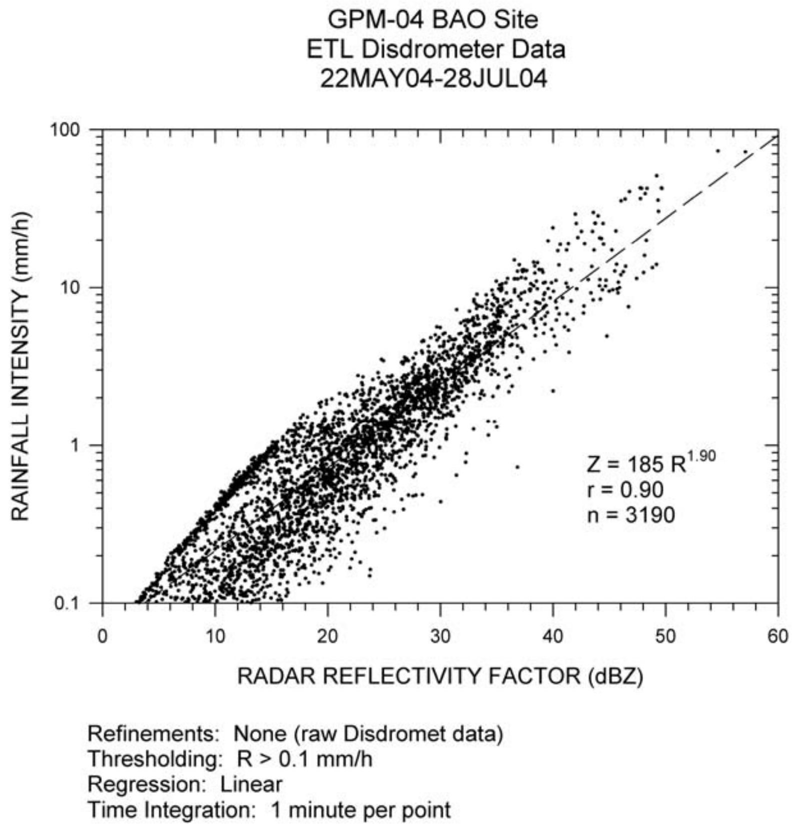

Figure 2. Scatter diagram and regression for the GPM04-Colorado disdrometer data for the case of no refinements, R as the dependent variable, a cutoff threshold of R > 0.1 mm/h, linear regression to log-R vs log-Z, and 1-minute accumulations of disdrometer data for each point. This is the reference case for the GPM04 dataset.

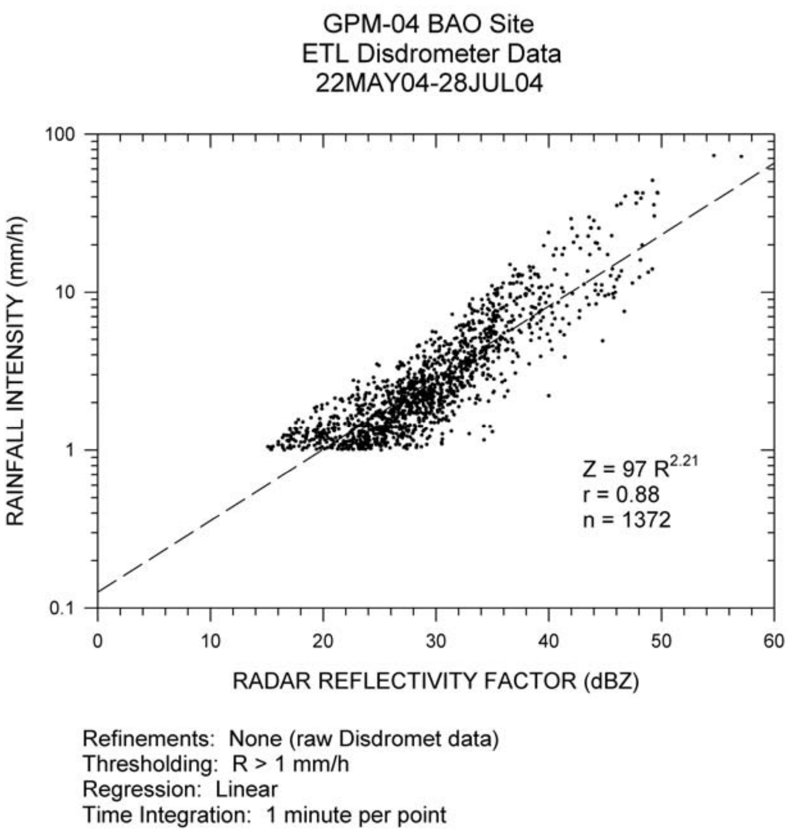

Figure 3. As in Figure 2, except the cut-off threshold is R > 1 mm/h.

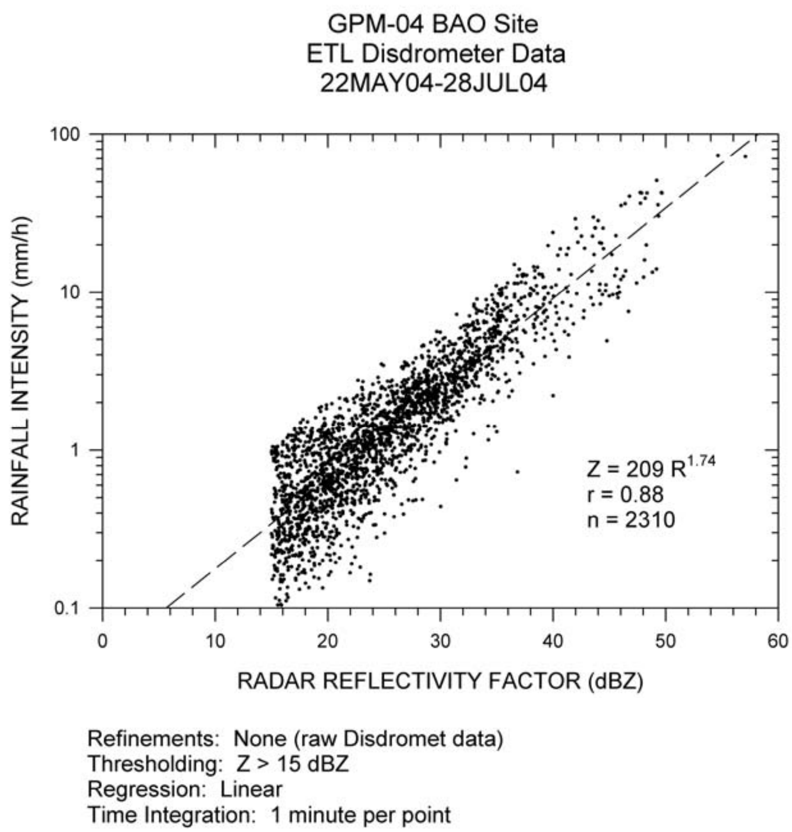

Figure 4. Same as in Figure 2, except the cut-off threshold is Z > 15 dBZ.

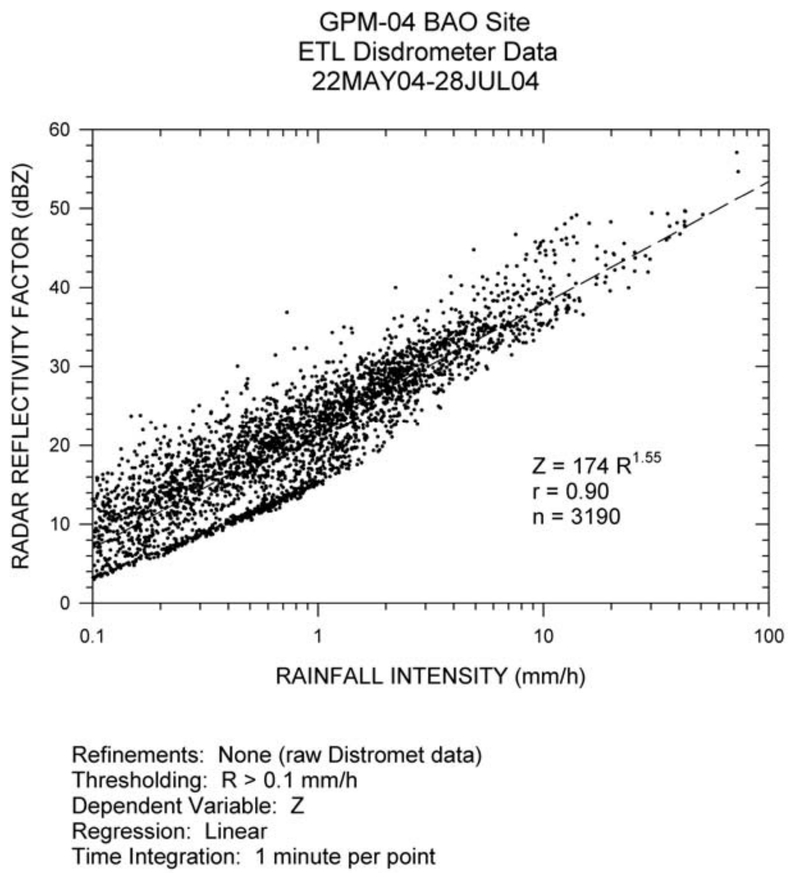

Figure 5. Same as in Figure 2, except Z is the dependent variable.

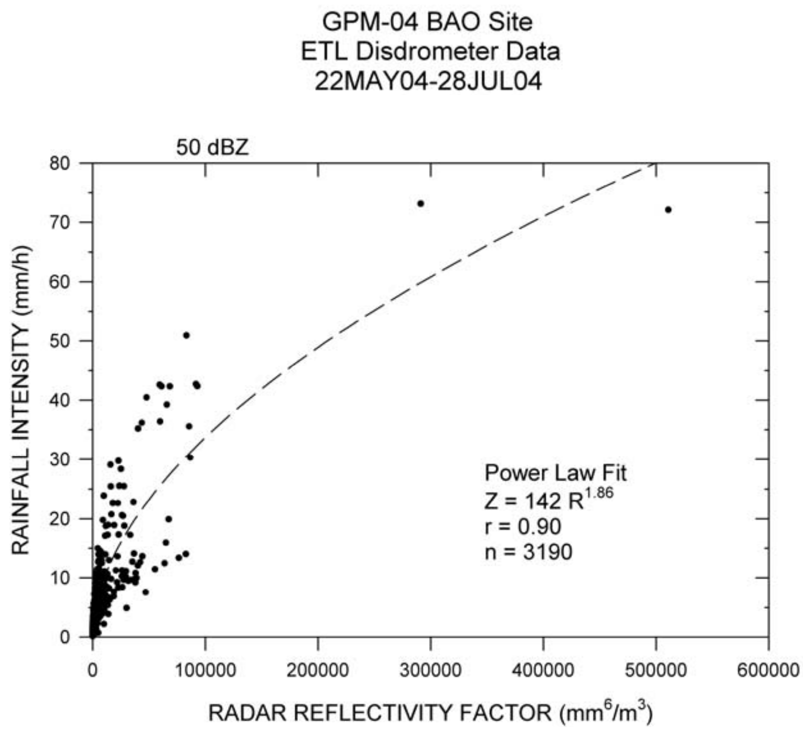

Refinements: None (raw Distromet data)
Thresholding: R > 0.1 mm/h
Dependent variable: R
Regression: 2-parameter power law
Time Integration: 1 minute per point

Figure 6. Same as in Figure 2, except the regression is a power law fit to R vs Z.

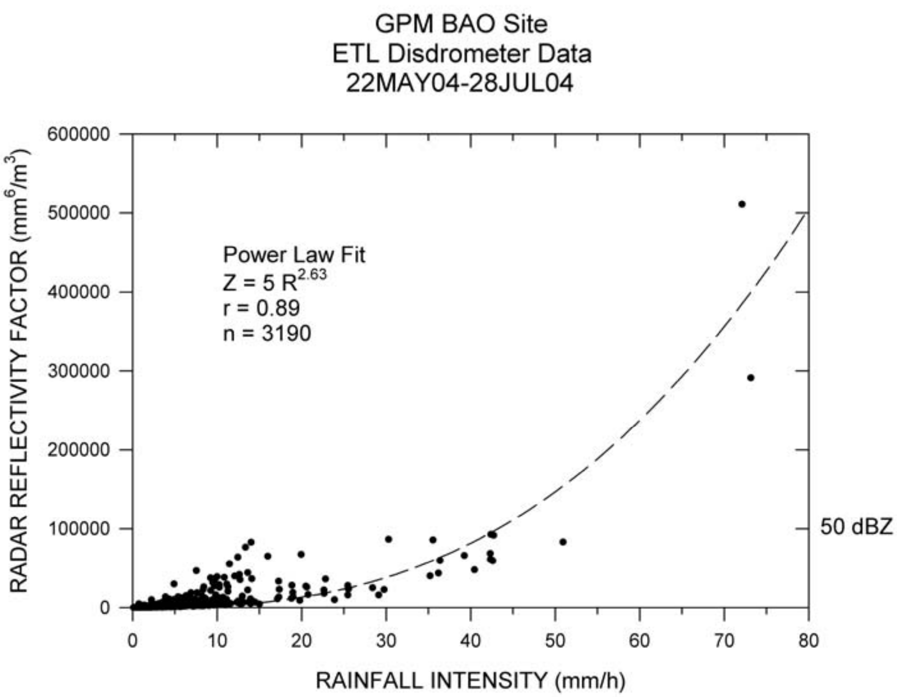

Refinements: None (raw Distromet data)
Thresholding: R > 0.1 mm/h
Dependent Variable: Z
Regression: 2-parameter power law
Time Integration: 1 minute per point

Figure 7. Same as in Figure 2, except Z is the dependent variable and the regression is a power law fit to Z vs R.

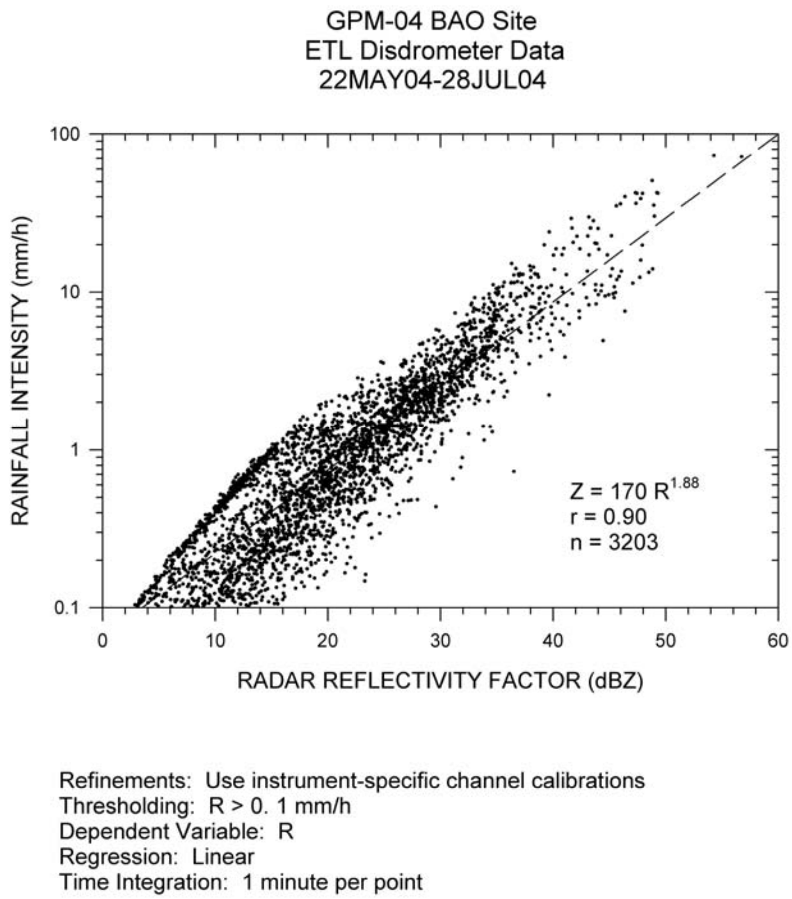

Figure 8. Same as in Figure 2, except the DSD data use the instrument-specific bin-drop diameter calibration instead of the nominal calibration.

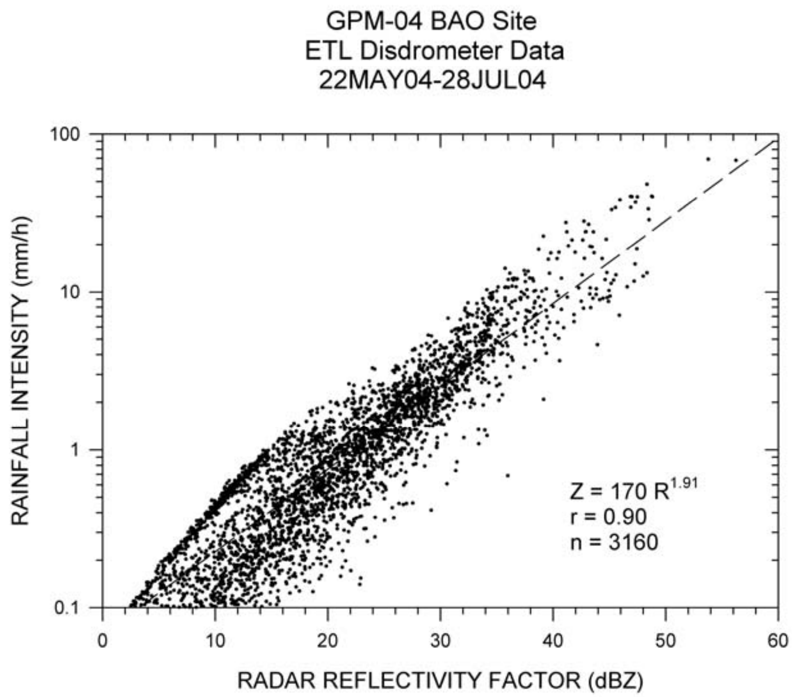

Refinements: Use altitude-corrected fall speeds
Thresholding: R > 0. 1 mm/h
Dependent Variable: R
Regression: Linear
Time Integration: 1 minute per point

Figure 9. Same as in Figure 2, except the DSD data have been adjusted for the drop fall speed and momentum-diameter relations for the 1600 m MSL altitude of the Colorado site.

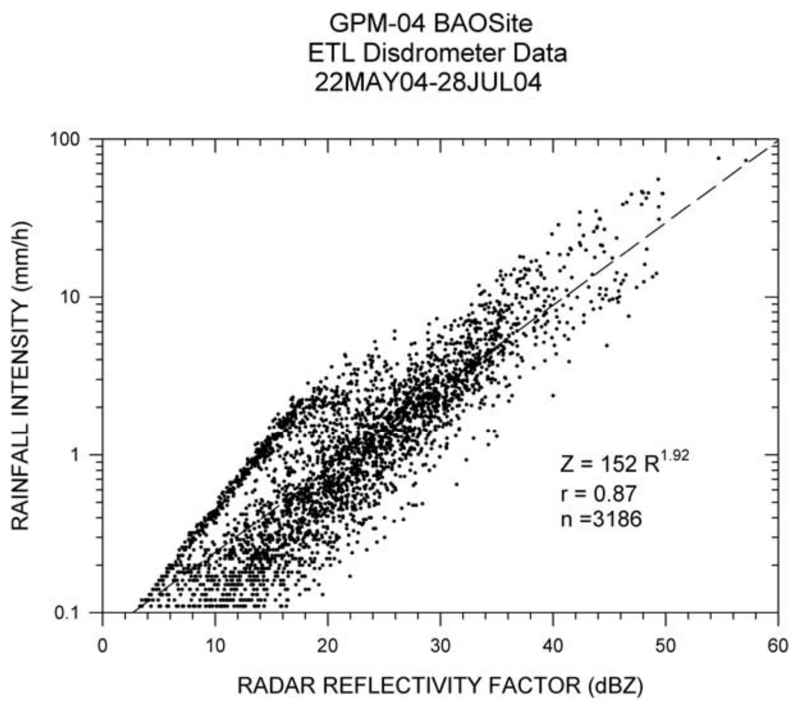

Refinements: Apply Dead-Time Corrections
Thresholding: R > 0.1 mm/h
Dependent Variable: R
Regression: Linear
Time Integration: 1 minute per point

Figure 10. Same as in Figure 2, except the DSD data have been adjusted for dead time corrections.

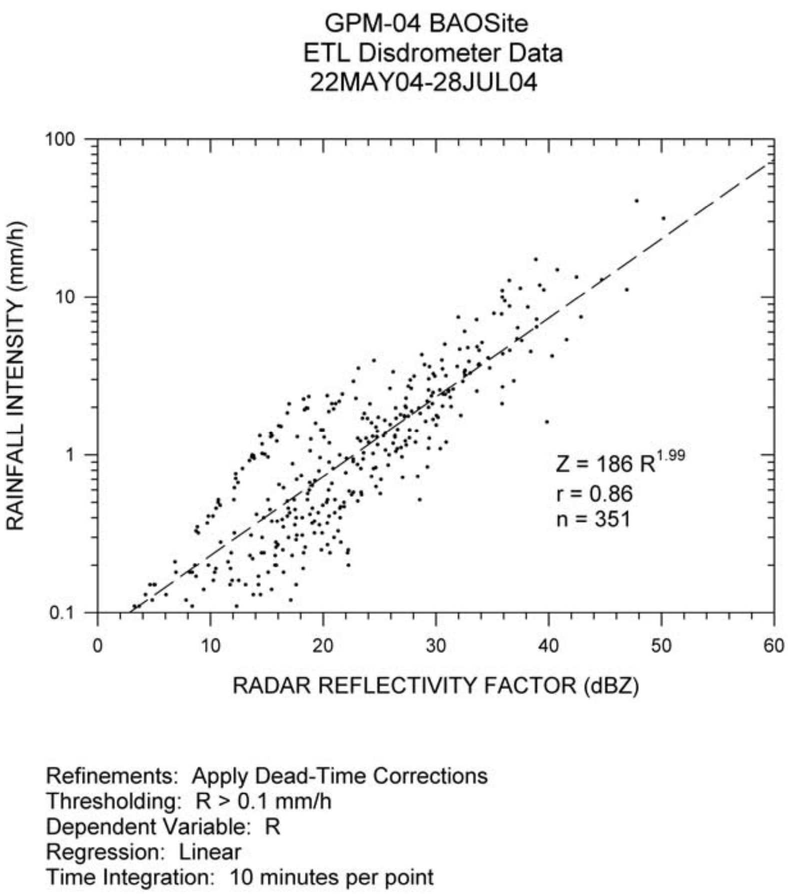

Figure 11. Same as in Figure 2, except the DSD data have been accumulated for 10 minutes with dead time corrections applied. Each point represents 10 minutes of disdrometer data.

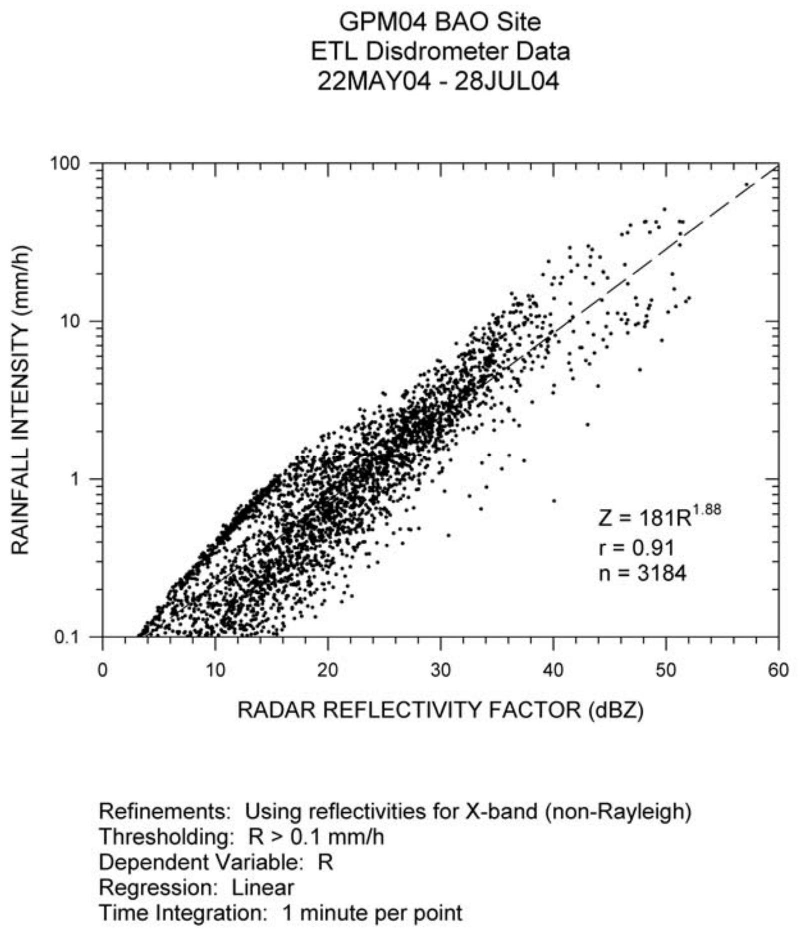

Figure 12. Same as in Figure 2, except the reflectivity factors computed from the DSD have been adjusted for the non-Rayleigh scattering conditions for observations with X-band wavelength radars.

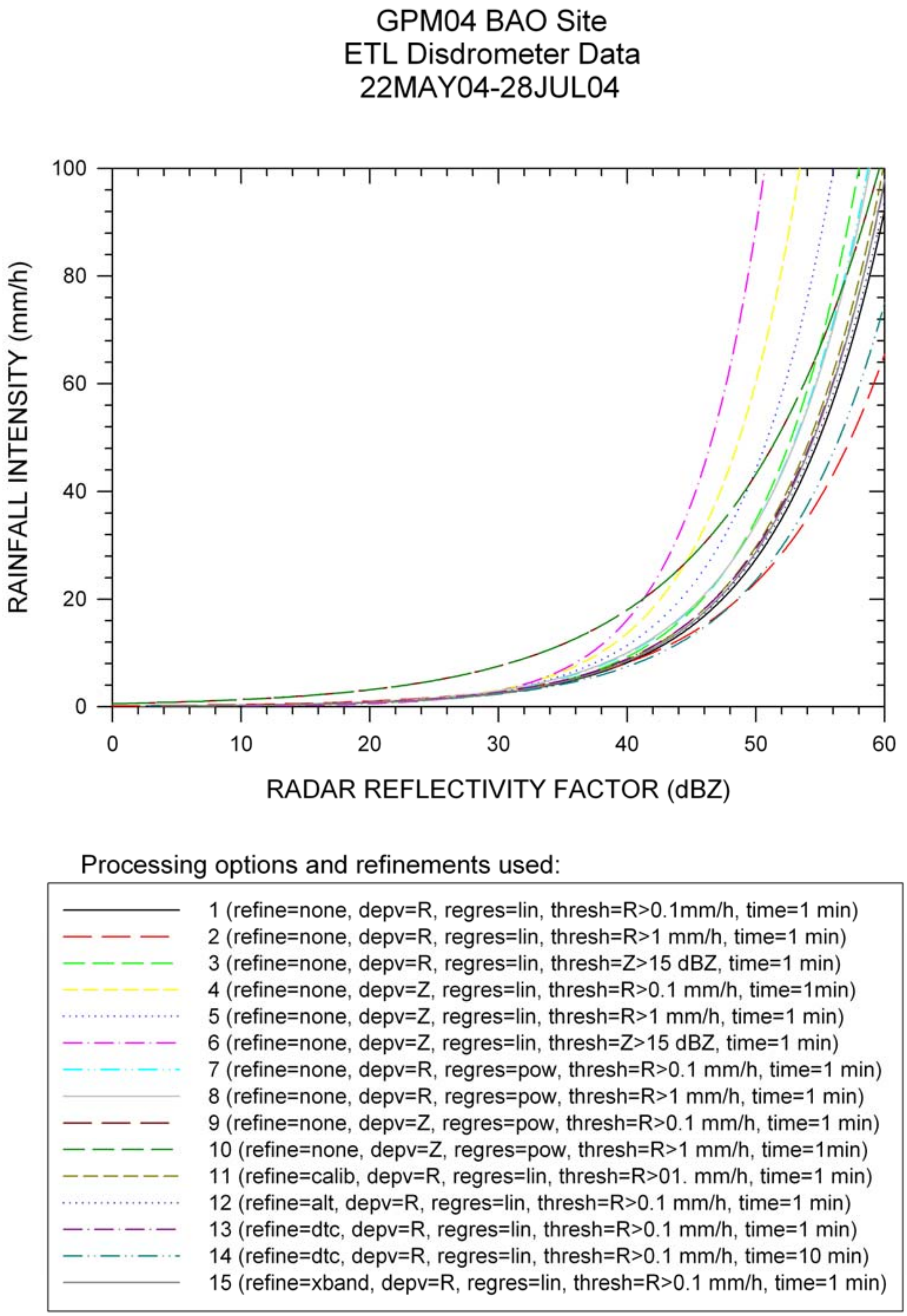

Figure 13. Graph of R vs Z showing the regressions derived from the same GPM04 dataset using various regression processing options and DSD refinements described in the text and shown on previous figures. The solid black line is for the reference situation shown in Figure 2.